Piezoceramics

DOI: 10.1002/anie.201202644

Polarization Rotation in the Monoclinic Perovskite $BiCo_{1-x}Fe_xO_3$**

Kengo Oka, Tsukasa Koyama, Tomoatsu Ozaaki, Shigeo Mori, Yuichi Shimakawa, and Masaki Azuma*

A piezoelectric ceramic, $Pb(Ti_{1-x}Zr_x)O_3$ (PZT), is widely used for various applications, such as transducers and sensors. PZT shows a maximum piezoelectric effect with a composition of about $x = 0.5$, the boundary separating the tetragonal *P*4*mm* (Ti-rich) and the rhombohedral *R*3*m* (Zr-rich) phases in the phase diagram. This boundary is known as a morphotropic phase boundary (MPB).[1] Investigation of the structural evolution at the MPB is indispensable for understanding the origin of the enhanced piezoelectric property in PZT. In 2000, Noheda reported the presence of a monoclinic phase at $x =$ 0.50 and 0.52 below 200 and 250 K, respectively, on the basis of powder synchrotron X-ray diffraction (SXRD) studies.[2] The monoclinic phase had a $\sqrt{2}a \times \sqrt{2}a \times a$ unit cell, where a was the cubic perovskite lattice parameter and the space group was *Cm*. This finding explains the mechanism of the piezoelectric enhancement as follows. The lack of a symmetry axis in the monoclinic structure allows the rotation of the ferroelectric polarization vector between the polar axes of the tetragonal and rhombohedral phases. This polarization rotation is induced by applying an electric field, leading to the enhancement of the piezoelectric constant.[3] Although the large piezoelectric response of PZT is successfully explained, the presence of a monoclinic phase in PZT as a distinct phase is controversial.[4] The insufficient difference in the pseudo cubic unit cell parameters of tetragonal, rhombohedral, and monoclinic phases inhibits the structural analysis based on diffraction studies. The *c*/*a* ratio of tetragonal (*P*4*mm*) $PbTi_{0.48}Zr_{0.52}O_3$ at 325 K is 1.01, which is quite close to unity, and the α of rhombohedral (*R*3*m*) $PbTi_{0.40}Zr_{0.60}O_3$ at 295 K is 90.45°,[2b] that is, almost orthogonal. The monoclinic phase has an intermediate structure between the tetragonal and the rhombohedral phases. These three phases are thus so close to cubic that their diffraction peaks overlap extremely.

Herein, we show the presence of a monoclinic $\sqrt{2}a \times \sqrt{2}a \times a$ structure with space group *Cm* as a single phase over a wide composition and temperature range in $BiCo_{1-x}Fe_xO_3$. The $BiCoO_3$–$BiFeO_3$ system attracts attention as a candidate for a lead-free piezoelectric material because of the similarity of the phase diagram to that of PZT.[5] The tetragonal and rhombohedral phases are adjacent at high temperature at around $x = 0.7$, and a monoclinic phase is found at room temperature in the vicinity of this composition. However, the space group and the precise crystal structure of this monoclinic phase remained unclear. The transition from a tetragonal to a rhombohedral structure was also predicted by a first-principles calculation by Diéguez et al., while the monoclinic phase is not stable in this calculation.[6] The present electron diffraction (ED) and SXRD studies consistently showed the presence of a *Cm* monoclinic phase as a single phase. Furthermore, polarization rotations between [001] and [111] directions of a pseudo cubic cell ($[001]_c$ and $[111]_c$, respectively) were found to be functions of composition and temperature.

The laboratory XRD patterns of $BiCo_{1-x}Fe_xO_3$ from $x =$ 0.60 to 0.72 are shown in Figure 1. Only the tetragonal phase was observed at $x = 0.60$, as reported previously. However,

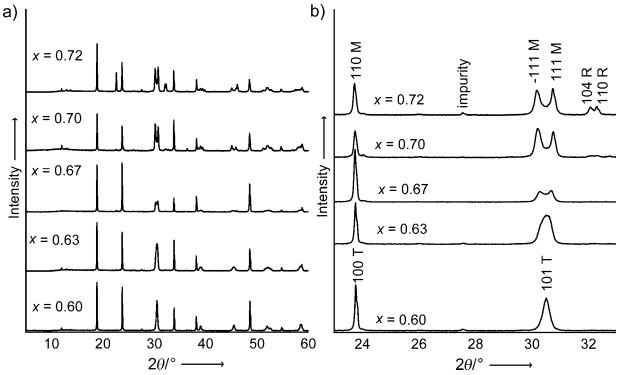

Figure 1. a) XRD patterns for $BiCo_{1-x}Fe_xO_3$ ($x = 0.60$, 0.63, 0.67, 0.70, and 0.72) collected at room temperature with CuKα radiation. b) Closer view of the XRD patterns. The suffixes R, T, and M after the indices represent rhombohedral, tetragonal, and monoclinic phases, respectively.

[*] Dr. K. Oka, Prof. Dr. M. Azuma
Materials and Structures Laboratory, Tokyo Institute of Technology
Nagatsuta, Midori, Yokohama, Kanagawa 226-8503 (Japan)
E-mail: koka@msl.titech.ac.jp
Dr. K. Oka, Prof. Dr. Y. Shimakawa, Prof. Dr. M. Azuma
Institute for Chemical Research, Kyoto University (Japan)
T. Koyama, T. Ozaaki, Prof. Dr. S. Mori
Department of Materials Science, Osaka Prefecture University (Japan)
Prof. Dr. S. Mori, Prof. Dr. Y. Shimakawa
Japan Science and Technology Agency (JST), CREST (Japan)

[**] We would like to thank Prof. H. Funakubo and Dr. S. Yasui (Tokyo Institute of Technology (Japan)) for their fruitful discussion. This work was partially supported by Grants-in-Aid from the Ministry of Education, Culture, Sports, Science and Technology (Japan) for Scientific Research (Nos. 19GS0207, 19340098, 19052008, 22244044), the Elements Science and Technology Project, the Cabinet Office of the Government of Japan through its "Funding Program for Next Generation World-Leading Researchers" (GR032), the Cooperative Research Project on Advanced Materials Development and Integration of Novel Structured Metallic and Inorganic Materials, and the Murata Science Foundation. The SXRD experiment was conducted at BL02B2 of SPring-8 with the approval of JASRI (2008B1750, 2009B1698, 2011A1258, and 2011B1896).

Supporting information for this article is available on the WWW under http://dx.doi.org/10.1002/anie.201202644.

the increase in $BiFeO_3$ content lead to the division of a 101 reflection into two. These peaks can be indexed as −111 and 111 reflections of the monoclinic phase with a $\sqrt{2}a \times \sqrt{2}a \times a$ unit cell. The structural change from the tetragonal *P*4*mm* to the monoclinic phase occurred gradually in a second-order manner. Further substitution led to the appearance of the rhombohedral *R*3*c* phase above $x = 0.70$. The single monoclinic phase was observed for the $x = 0.63$ and 0.67 samples. The structural transition from the monoclinic to the rhombohedral phases was first-order in accordance with the 9% gap in the pseudo cubic unit-cell volume. These behaviors are different from that of PZT, where the structural transition from the tetragonal *P*4*mm* to the rhombohedral *R*3*m* via monoclinic *Cm* phases occurs continuously. Another difference from PZT is that the rhombohedral phase of $BiCo_{1-x}Fe_xO_3$ has the space group *R*3*c*, which is present in PZT as the low temperature phase of *R*3*m* phase.[7] The transition from *R*3*m* to *R*3*c* originates from the tilting of the $(Zn,Ti)O_6$ octahedra, leading to the doubling in the *c* axis.

The ED patterns shown in Figure 2 confirmed the $\sqrt{2}a \times \sqrt{2}a \times a$ unit cell and *Cm* space group of the monoclinic phase. The composition dependence of the lattice parameters of the monoclinic *Cm* phase is shown in Figure 3. The lattice parameters increased gradually as Fe content increased owing to the larger ionic radius of Fe compared to that of Co (Co^{3+} 0.61 Å, Fe^{3+} 0.65 Å).[8] The monoclinic angle β also increased with *x*. It appears strange that the changes in lattice parameters continued after the separation into monoclinic and rhombohedral phases took place, which is probably because both the monoclinic and the rhombohedral phases had the same $GdFeO_3$-type high-pressure structure.[9] When the sample was prepared under high-pressure conditions, only a $GdFeO_3$-type structure was present, which transformed into monoclinic and rhombohedral phases when the pressure was

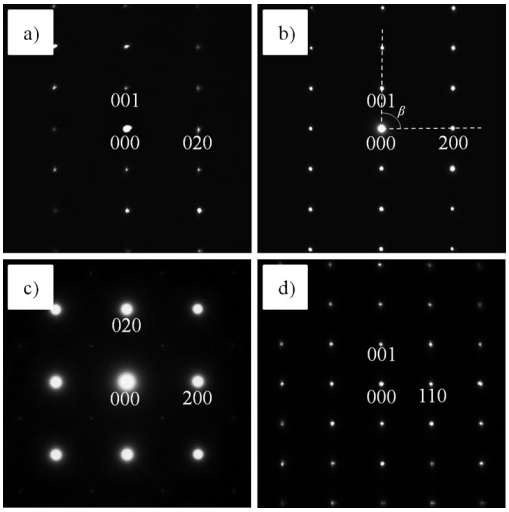

Figure 2. a) [100], b) [010], c) [001], and d) [−110] zone-axis selected-area electron diffraction patterns obtained for $BiFe_{0.30}Co_{0.70}O_3$ at 298 K. The electron diffraction spots are indexed on the cubic perovskite structure. The monoclinic angle β can be estimated to be approximately 91.4° in the reciprocal lattice space. The space group is deduced to be *Cm* from the analysis of various ED patterns. The unit cell is $\sqrt{2}a \times \sqrt{2}a \times a$, where *a* represents the lattice parameter of the cubic perovskite structure.

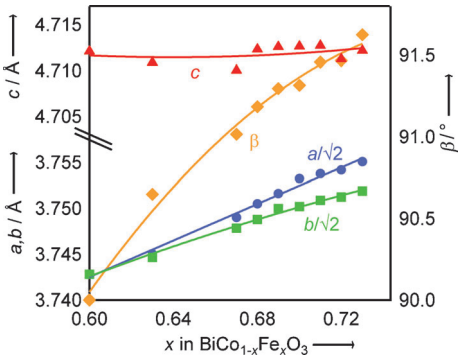

Figure 3. The composition dependence of the lattice parameters of monoclinic $BiCo_{1-x}Fe_xO_3$ ($0.60 \le x \le 0.73$).

reduced. In this room-temperature process, no ionic diffusion that causes the compositional phase separation took place. We note that such coexistence of two phases with the same composition is often found in oxides.[10]

For further investigation, we performed a Rietveld analysis of the SXRD patterns of $x = 0.63$, 0.70, and 0.72 samples. The fittings successfully converged, assuming the mixing of monoclinic and rhombohedral phases, and the results are summarized in Figure 4 and the Supporting Information, Table S1. The refined crystal structure of monoclinic $BiCo_{1-x}Fe_xO_3$ ($x = 0.63$, 0.70, and 0.72) was closely related with its parent compound, tetragonal $BiCoO_3$, where the ordering of the d_{xy} orbital lead to the CoO_5 pyramidal coordination and a large spontaneous polarization of 120 $\mu C\,cm^{-2}$ was calculated by assuming a point-charge model.[9] Monoclinic $BiCo_{1-x}Fe_xO_3$ preserved the large polar distortion, and the spontaneous polarizations calculated were 121 $\mu C\,cm^{-2}$ for $x = 0.63$, 117 $\mu C\,cm^{-2}$ for $x = 0.70$, and 117 $\mu C\,cm^{-2}$ for $x = 0.72$, which are about twice as large as that reported for $PbZr_{0.52}Ti_{0.48}O_3$ at 20 K (54 $\mu C\,cm^{-2}$).[2b] The polarization vector of the tetragonal *P*4*mm* phase pointed toward the $[001]_c$ direction, and that of the rhombohedral *R*3*m* phase pointed toward the $[111]_c$ direction. We denote $[001]_c$ as the direction perpendicular to the $(001)_c$ plane. The polarization in the monoclinic *Cm* phase was in a $(110)_c$ plane, between the $[001]_c$ and $[111]_c$ directions. Doubling of the unit cell, $\sqrt{2}a \times \sqrt{2}a \times a$ as shown in Figure 4b), was required to tilt the polarization direction from the $[001]_c$ direction to the $[111]_c$ direction. The polarization direction reported for $PbZr_{0.52}Ti_{0.48}O_3$ at 20 K tilted 24° from the $[001]_c$ direction.[2b] In monoclinic $BiCo_{1-x}Fe_xO_3$, the tilting angles were 2° for $x = 0.63$, 12° for $x = 0.70$, and 17° for $x = 0.72$ (Figure 5). Note that the polarization tilts in the opposite direction to the monoclinic distortion. The tilting angles from the monoclinic $[001]_m$ directions were 2.9° for $x = 0.63$, 13.4° for $x = 0.70$, and 18.5° for $x = 0.72$. Owing to the large distortion along the $[001]_c$ direction, the directions of the polarization were closer to the $[001]_c$ direction compared with that of PZT. The angle from the $[001]_c$ direction increased as the Fe content increased, indicting the continuous change of the polarization direction. It should be noted that this is the first observation of the polarization rotation predicted for a monoclinic perovskite.

The thermal stability of the monoclinic phase was also investigated. Figure 6 shows the temperature dependence of the SXRD pattern of $BiCo_{0.30}Co_{0.70}O_3$. A second-order

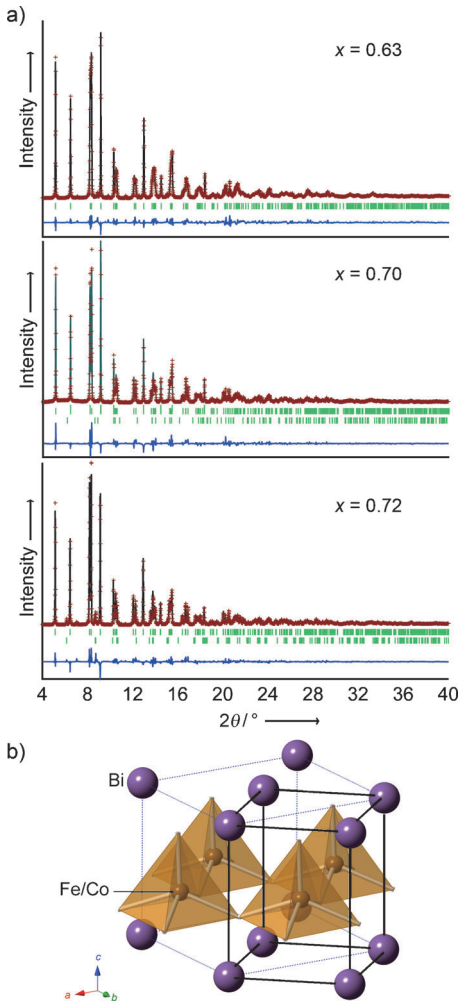

Figure 4. a) SXRD patterns of $BiCo_{1-x}Fe_xCoO_3$ at room temperature and the results of Rietveld fits. The wave lengths λ are 0.42335 Å, 0.42290 Å, and 0.42309 Å for $x = 0.63$, 0.70, and 0.72, respectively. Observed (red, +), calculated (black line), and difference profiles (blue line) are shown together with Bragg marks (green) for the monoclinic (upper) and rhombohedral (lower) phases. b) The crystal structure of monoclinic $BiCo_{0.30}Fe_{0.70}CoO_3$. Broken and solid lines represent the monoclinic and pseudo cubic unit cells, respectively.

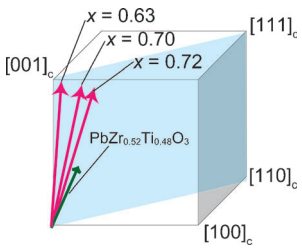

Figure 5. The polarization vectors of the monoclinic *Cm* phase of $BiCo_{1-x}Fe_xO_3$ ($x = 0.63$, 0.70, and 0.72) at 300 K and $PbZr_{0.52}Ti_{0.48}O_3$ at 20 K.[2b] The indices $[001]_c$, $[100]_c$, $[110]_c$, and $[111]_c$ are based on the pseudo cubic unit cell.

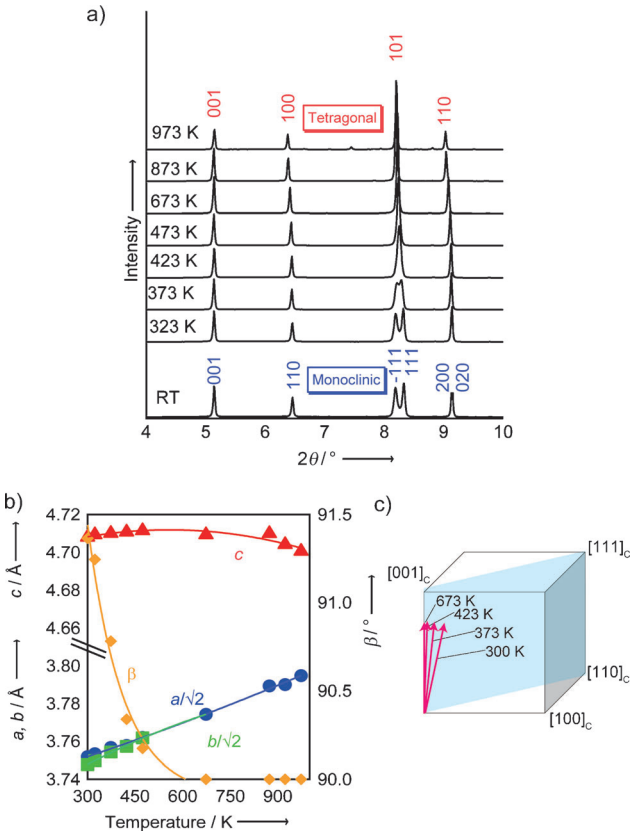

Figure 6. a) SXRD patterns of $BiCo_{0.30}Fe_{0.70}O_3$ at elevated temperatures ($\lambda = 0.4229$ Å). b) The temperature dependence of the lattice parameters of monoclinic $BiCo_{0.30}Fe_{0.70}O_3$. c) Temperature dependence of the monoclinic distortion angle β. The inset illustrates the polarization vector, which indicates the temperature-induced polarization rotation.

structural transition from monoclinic *Cm* to tetragonal *P4mm* structures at high-temperature, as reported for PZT,[2b] was observed. This behavior also suggests that the monoclinic *Cm* phase was derived from the tetragonal *P4mm* phase, not from the rhombohedral *R3c* phase. The monoclinic distortion angle β decreased gradually during heating and settled at 90° above 673 K, indicating the completion of the structural transition. Further heating led to the decomposition of the sample above 973 K. The tilting angles from the $[001]_c$ direction were 12° at 300 K, 6° at 373 K, 2° at 423 K, and 0° at 673 K. The above result clearly shows that the polarization rotation also took place during heating.

In conclusion, the present study indicates that polarization rotates as functions of composition and temperature. An enhancement of piezoelectric property is expected if such rotation is induced by applying an electric field, as suggested for PZT. Unfortunately, no monoclinic $BiCo_{1-x}Fe_xO_3$ sample resistive enough for the piezoelectric measurement has been prepared, either in bulk or thin film forms. However, similar monoclinic phases were recently found in other bismuth-containing perovskite systems, such as $BiAl_{0.75}Ga_{0.25}O_3$.[11] Both structural and electrical investigations of these materials will experimentally clarify the relationship between the crystal structure and the piezoelectric properties.

Experimental Section

Polycrystalline $BiCo_{1-x}Fe_xO_3$ samples were prepared with a cubic anvil-type high-pressure apparatus. Stoichiometric mixtures of Bi_2O_3, Co_3O_4, and Fe_2O_3 were sealed in an Au capsule with 10 mg of $KClO_4$ and treated at 4 GPa and 1000 °C for 30 min. The obtained powder was washed with distilled water to remove the residual KCl. The XRD patterns were collected with a Bruker D8 ADVANCE diffractometer for phase identification and refinement of the lattice parameters. The data were analyzed by the Rietveld method with the software TOPAS (Bruker AXS, Karlsruhe, Germany). ED experiments were carried out at 298 K by using JEOL JEM-2010 transmission electron microscopy (TEM) equipped with a double-tilting holder. The space group of the monoclinic phase was deduced by obtaining various electron diffractions at 298 K. The SXRD patterns were collected with a large Debye–Scherrer camera installed at the BL02B2 beam line of SPring-8[12] and analyzed by using RIETAN-2000[13] programs.

Received: April 5, 2012
Published online: July 2, 2012

Keywords: high-pressure synthesis · perovskite phases · piezoceramics · X-ray diffraction

[1] B. Jaffe, W. R. Cook, H. Jaffe, *Piezoelectric ceramics*, Academic Press, New York, **1971**, pp. 148 – 183.
[2] a) B. Noheda, D. E. Cox, G. Shirane, J. A. Gonzalo, L. E. Cross, S. E. Park, *Appl. Phys. Lett.* **1999**, *74*, 2059 – 2061; b) B. Noheda, J. A. Gonzalo, L. E. Cross, R. Guo, S. E. Park, D. E. Cox, G. Shirane, *Phys. Rev. B* **2000**, *61*, 8687 – 8695.
[3] a) L. Bellaiche, A. García, D. Vanderbilt, *Phys. Rev. Lett.* **2000**, *84*, 5427 – 5430; b) D. Vanderbilt, M. H. Cohen, *Phys. Rev. B* **2001**, *63*, 094108.
[4] a) R. Ragini, S. K. Mishra, D. Pandey, H. Lemmens, G. V. Tendeloo, *Phys. Rev. B* **2001**, *64*, 054101; b) D. M. Hatch, H. T. Stokes, R. Ranjan, R. Ragini, S. K. Mishra, D. Pandey, B. J. Kennedy, *Phys. Rev. B* **2002**, *65*, 212101; c) A. M. Glazer, P. A. Thomas, K. Z. Baba-Kishi, G. K. H. Pang, C. W. Tai, *Phys. Rev. B* **2004**, *70*, 184123; d) K. A. Schönau, L. A. Schmitt, M. Knapp, H. Fuess, R. A. Eichel, H. Kungl, M. J. Hoffmann, *Phys. Rev. B* **2007**, *75*, 184117; e) T. Asada, Y. Koyama, *Phys. Rev. B* **2007**, *75*, 214111; f) D. E. Cox, B. Noheda, G. Shirane, *Phys. Rev. B* **2005**, *71*, 134110; g) J. Frantti, S. Ivanov, S. Eriksson, H. Rundlöf, V. Lantto, J. Lappalainen, M. Kakihana, *Phys. Rev. B* **2002**, *66*, 064108; h) R. Ragini, R. Ranjan, S. K. Mishra, D. Pandey, *J. Appl. Phys.* **2002**, *92*, 3266 – 3274.
[5] a) M. Azuma, S. Niitaka, N. Hayashi, K. Oka, M. Takano, H. Funakubo, Y. Shimakawa, *Jpn. J. Appl. Phys.* **2008**, *47*, 7579 – 7581; b) Y. Nakamura, M. Kawai, M. Azuma, Y. Shimakawa, *Jpn. J. Appl. Phys.* **2010**, *49*, 051501; c) Y. Nakamura, M. Kawai, M. Azuma, M. Kubota, M. Shimada, T. Aiba, Y. Shimakawa, *Jpn. J. Appl. Phys.* **2011**, *50*, 031505; d) S. Yasui, K. Nishida, H. Naganuma, S. Okamura, T. Iijima, H. Funakubo, *Jpn. J. Appl. Phys.* **2007**, *46*, 6948 – 6951; e) S. Yasui, O. Sakata, M. Nakajima, S. Utsugi, K. Yazawa, T. Yamada, H. Funakubo, *Jpn. J. Appl. Phys.* **2009**, *48*, 09KD06.
[6] O. Diéguez, J. Íñiguez, *Phys. Rev. Lett.* **2011**, *107*, 057601.
[7] C. Michel, J.-M. Moreau, G. D. Achenbach, R. Gerson, W. J. James, *Solid State Commun.* **1969**, *7*, 865 – 868.
[8] R. D. Shannon, *Acta Crystallogr. Sect. A* **1976**, *32*, 751 – 767.
[9] K. Oka, M. Azuma, W. Chen, H. Yusa, A. Belik, E. Takayama-Muromachi, M. Mizumaki, N. Ishimatsu, N. Hiraoka, M. Tsujimoto, M. Tucker, J. Attfield, Y. Shimakawa, *J. Am. Chem. Soc.* **2010**, *132*, 9438 – 9443.
[10] M. Azuma, W. T. Chen, H. Seki, M. Czapski, S. Olga, K. Oka, M. Mizumaki, T. Watanuki, N. Ishimatsu, N. Kawamura, S. Ishiwata, M. G. Tucker, Y. Shimakawa, J. P. Attfield, *Nat. Commun.* **2011**, *2*, 347.
[11] A. A. Belik, T. Wuernisha, T. Kamiyama, K. Mori, M. Maie, T. Nagai, Y. Matsui, E. Takayama-Muromachi, *Chem. Mater.* **2006**, *18*, 133 – 139.
[12] E. Nishibori, M. Takata, K. Kato, M. Sakata, Y. Kubota, S. Aoyagi, Y. Kuroiwa, M. Yamakata, N. Ikeda, *Nucl. Instrum. Methods Phys. Res. Sect. A* **2001**, *467*, 1045 – 1048.
[13] F. Izumi, T. Ikeda, *Mater. Sci. Forum* **2000**, *321 – 3*, 198 – 203.

